

EVOLUTION OF REYNOLDS STRESSES IN TURBULENT WAKE-FLOWS WITH LONGITUDINAL PRESSURE GRADIENT

J. W. ELSNER and J. WILCZYŃSKI (CZĘSTOCHOWA)

The report presented here deals with the theoretical as well as experimental analysis of the development of Reynolds stresses in shear flows with longitudinal pressure gradients. The obtained results have pointed out that the negative pressure gradient accelerates the mean velocity field equalization and damps the turbulent fluctuations of the flowing medium. The positive value of $\partial\bar{p}/\partial x_1$ brings about the growth of the overall turbulence level which is probably due to an increase of energy-flux transferred from the mean to the turbulent motion. Special importance has also been attached to the analysis of energy spectrum functions and their dependence on longitudinal pressure gradient. The spectral coefficient of double correlation between turbulent velocity components has been found to be an increasing function of $\partial\bar{p}/\partial x_1$, which may be treated as a tendency of accelerated flows to a more intensive stabilization of isotropic structure.

1. INTRODUCTION

The set of problems concerning turbulent wake-flows belong undoubtedly to one of the most interesting parts of contemporary fluid mechanics. The evolution of velocity field behind a single isolated body has been the subject of many intensive studies. Some of those dealt with the influence exerted on the wake-flow by the impulsive (for example, [1] and [2]) or continuous [3] longitudinal pressure gradient. Far less numerous are those works which concern the flow pattern behind the cascade profiles immersed in a flowing medium. This question was first investigated by GRAN OLSON [4] and, later, by STEWARD [5], SATO [6], TAMAKI and OSHIMA [7], ELSNER [8, 9, 10] and others. However, none of the studies mentioned above analyzed the turbulence structure in accelerated or in retarded cascade wake-flows.

The report presented here deals with the results of empirical investigations carried out at the Institute of Heat Machinery at the Technical University of Częstochowa. Research was begun so as to explain to what extent the evolution of Reynolds stresses in turbulent wake-flows may be affected by the longitudinal pressure gradient of a constant value in a downstream direction.

2. SEMI-PRESERVATION ANALYSIS

Let us now consider whether the semi-preserving solutions — in the sense formulated for the first time in works [9] and [10] — can be found for the cascade wake-flows with arbitrary, longitudinal pressure gradients.

At a sufficiently far distance behind the cascade, the equation governing the development of a two-dimensional, incompressible turbulent wake, with the quantities of the second order being neglected and the static pressure uniformed at every stream-wise cross section, may be written in the form

$$(2.1) \quad U_1 \frac{\partial U_1}{\partial x_1} + \frac{\partial}{\partial x_2} \overline{u_1 u_2} + \frac{1}{\rho} \frac{dp}{dx_1} = 0.$$

To describe the overall velocity field in a semi-preserving region of the cascade-flow, let us introduce the relations

$$(2.2) \quad \begin{aligned} U_1 &= U_s(x_1) - \Delta U_m f(\eta), \\ \overline{u_1^2} &= u_*^2 \varphi(\eta), \\ \overline{u_2^2} &= u_*^2 \psi(\eta), \\ \overline{u_1 u_2} &= \tau_* \lambda(\eta), \end{aligned}$$

where

$$(2.3) \quad U_s(x_1) = \frac{1}{l(x_1)} \int_0^{l(x_1)} U_1(x_1, x_2) dx_2 = \frac{U_\infty t}{l(x_1)}$$

stands for a space averaged value of velocity determined from the continuity equation and, $\eta = x_2/l(x_1)$ is a new relative coordinate. The quantities l , ΔU_m , u_* and τ_* are suitably chosen local scales; first, once of them (concerning the mean velocity field) have been interpreted in Fig. 1.

It is worth emphasizing that contrary to the conception of self-preservation (or self-similarity) as formulated by TOWNSEND [11] and applied to the plane wake, for example, by NARASIMHA and PRABHU [1], the scales mentioned above are inter-related so that their ratios

$$(2.4) \quad \frac{\Delta U_m}{u_*}, \quad \frac{\Delta U_m}{\tau_*^{1/2}}, \quad \frac{\tau_*}{u_*^2}$$

are not independent of the coordinate x_1 being the certain explicit functions of the distance from the cascade.

In particular, the scales τ_* and u_* are mutually connected by means of a correlation coefficient which, for 2D-flow, takes the form

$$(2.5) \quad R_{12} = \frac{\overline{u_1 u_2}}{(\overline{u_1^2} \overline{u_2^2})^{1/2}} = \frac{\tau_*}{u_*^2} \frac{\lambda(\eta)}{[\varphi(\eta) \psi(\eta)]^{1/2}} = R_{12 \max}(\bar{x}_1) F(\eta).$$

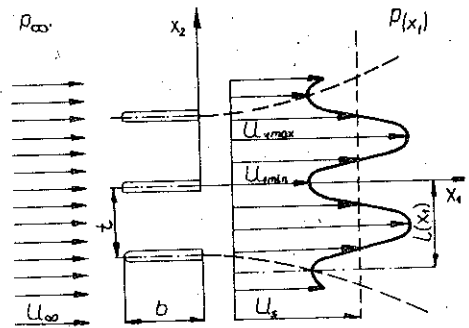


FIG. 1. Mean velocity field behind the cascade plates.

According to the detailed analysis presented in [12] for the type of flow considered here

$$(2.6) \quad \frac{1}{\rho} \frac{dp}{dx_1} = -U_s \frac{dU_s}{dx_1}.$$

Now, substituting Eqs. (2.2), (2.3) and (2.6) in Eq. (2.1) we obtain

$$(2.7) \quad \frac{1}{\tau_*} \left[\frac{d(\Delta U_m)}{dx_1} + \frac{f' \eta}{f} \frac{\Delta U_m}{U_s} \frac{dU_s}{dx_1} \right] = \frac{\lambda'}{t U_\infty f}$$

where derivatives f' and λ' have been calculated with respect to the relative coordinate η .

The region in which Eqs. (2.2) and (2.7) are simultaneously fulfilled for all the streamwise cross-sections has been called in [9] and [10] a semipreserving region of cascade flow.

Under such circumstances there ought to be of course

$$(2.8) \quad \frac{1}{\tau_*} \frac{d(\Delta U_m)}{dx_1} = \text{const}, \quad \frac{1}{\tau_*} \frac{\Delta U_m}{U_s} \frac{dU_s}{dx_1} = \text{const}.$$

Let us now assume that according to the numerous experimental proofs, the velocity scales ΔU_m and u_* appear to be the power functions of the distance from the cascade, that is

$$(2.9) \quad \Delta U_m \sim x_1^{-\kappa}, \quad u_* \sim x_1^{-k}.$$

Introducing Eq. (2.9) to Eq. (2.8) gives

$$(2.10) \quad \begin{aligned} U_s &\sim x_1^c, & l &\sim x_1^{-c}, \\ \tau_* &\sim x_1^{-(\kappa+1)}, & R_{12} &\sim x_1^{2k-(\kappa+1)}. \end{aligned}$$

The general tendency towards the stabilization of isotropic structure as observed in the majority of turbulent flows, demands that the coefficient R_{12} be the decreasing function of the coordinate x_1 , which is equivalent with the condition formulated in [10]

$$(2.11) \quad 2k < (\kappa + 1).$$

However, it should be stressed that the semi-preserving conditions could not be achieved in cascade-wake flows having a constant different from zero longitudinal pressure gradient in a down-stream direction. This issues directly from the fact that in this case there is no possibility for both relations (2.6) and (2.8) to be fulfilled at the same time.

3. EXPERIMENTAL DETAILS

According to the conception presented above the semi-preserving conditions of cascade-flow may be achieved (beyond the case $\partial p/\partial x_1 = 0$) only when the longitudinal pressure gradient shows the power-functional dependence on the coordinate x_1 . As it has already been emphasized, the aim of this report is to find the influence exerted by $\partial p/\partial x_1$ on the components of the turbulent stress-tensor. For the quantitative description of this effect it was necessary to maintain a constant value of $\partial p/\partial x_1$ along the whole length of the measuring section while the experiment was being performed.

The experiment was carried out in a low-speed, open circuit cascade-tunnel in a wake-flow behind the row of parallel flat plates, shown schematically in Fig. 2. The initial turbulence of incoming flow was generated by means of special grids

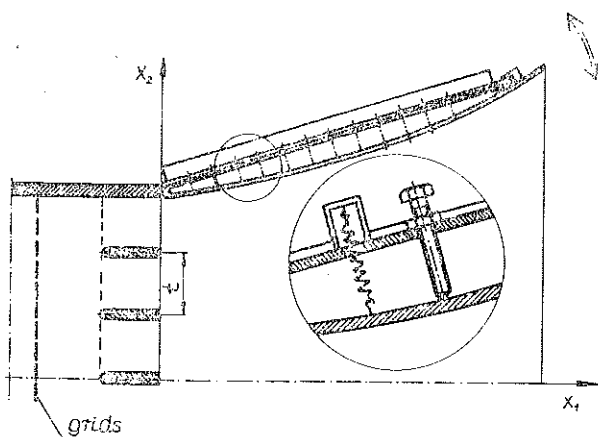


FIG. 2. Measuring section of the wind-tunnel.

installed in a channel upstream of the plates. The regulation of the distance between the grids and the inlet edges of the plates allowed to obtain the variation of the initial turbulence level up to 10%.

The flexible top and bottom walls of the outlet channel were formed and adjusted in such a way as to achieve a constant value of a pressure gradient in the downstream direction.

The velocity field in a wake-flow was examined by means of two DISA hot-wire anemometers (CTA-55M System) and a set-up of time correlation analyzer. The block diagram of the measuring equipment applied in the analysis of turbulence signals is shown in Fig. 3. The traversing mechanism of a hot-sensor was electrically connected with a XY-recorder which made it possible to get its response in the form of a graphical plot.

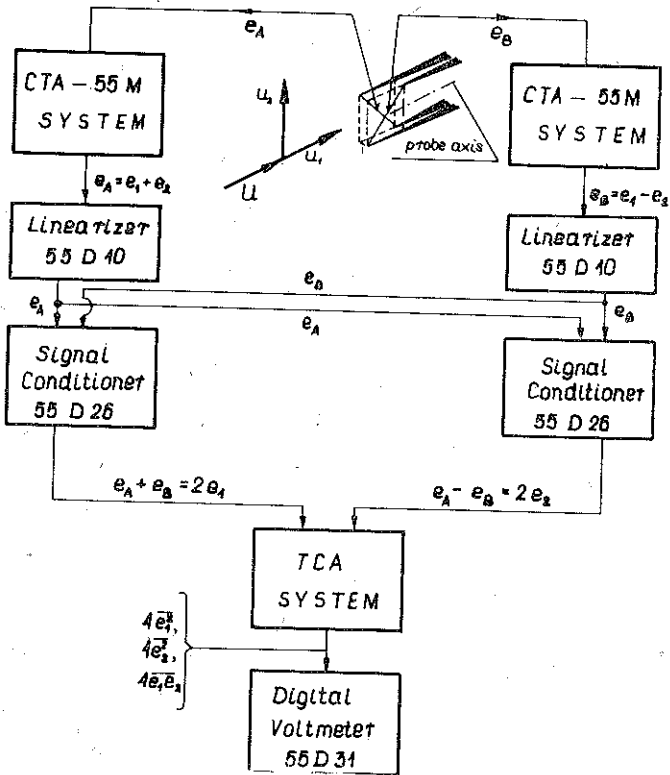


FIG. 3. Block diagram of the measuring system.

3.1. Empirical results

The typical flow pattern in the region of its periodicity that is downstream of the three middle cascade plates is shown in Fig. 1.

Considering the process of mean velocity field equilization it is convenient to introduce the notion of the degree of mean flow non-uniformity as defined by the relation

$$(3.1) \quad \beta(x_1) = \frac{U_{1 \max} - U_{1 \min}}{2U_\infty} = \frac{\Delta U_m}{2U_\infty}$$

Here, the quantity ΔU_m designates the maximum difference of mean flow velocity in a given \bar{x}_1 plane; U_∞ was already defined by Eq. (2.3)

The evolution of parameter β in the downstream direction is demonstrated in Fig. 4. As it can be seen in a certain distance behind the plates, β becomes a power function of the coordinate \bar{x}_1

$$\beta(x_1) \sim \bar{x}_1^{-\kappa}$$

with the exponent κ depending on the value of the longitudinal pressure gradient

$$(3.2) \quad \Phi = \frac{\partial \bar{p}}{\partial \bar{x}_1} = \frac{\partial \left(\frac{p - p_\infty}{0.5 \rho U_\infty^2} \right)}{\partial (x_1/t)}$$

The results presented here show clearly that the process of mean velocity field equalization is more intensive in accelerated flows than in retarded ones; the negative pressure gradient is then the factor which causes intensified mean-flow uniformity.

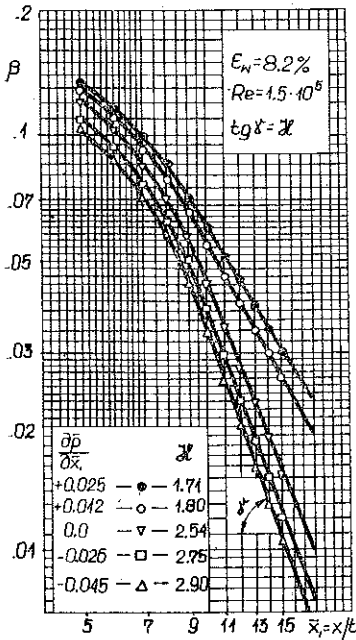


FIG. 4. Degree of mean flow non-uniformity as a function of the coordinate \bar{x}_1 .

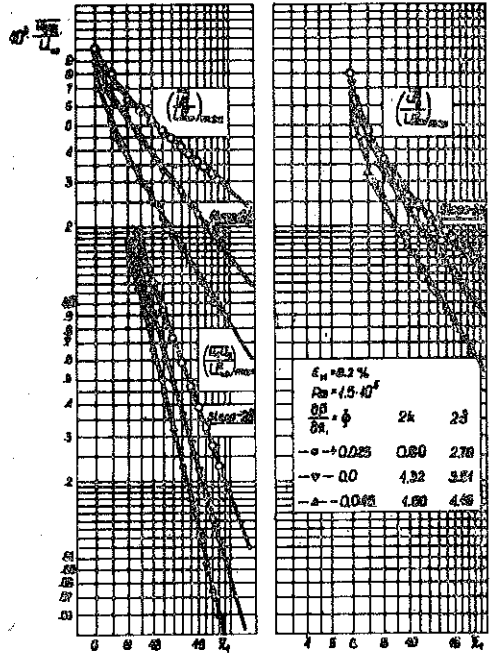


FIG. 5. Evolution of turbulence stresses in a downstream direction.

The evolution of Reynolds stresses in flows with different pressure gradients may be estimated on the base of empirical data presented in Fig. 5, comprising normal as well as shear components of turbulent stress tensor, respectively. By analogy to the results previously discussed it is worth noticing that at some distance from the cascade plates all the curves plotted here show power-law dependence on the variable \bar{x}_1 .

$$\overline{u_1^2} \sim \overline{u_2^2} \sim \bar{x}_1^{-2k}, \quad \overline{u_1 u_2} \sim \bar{x}_1^{-2\delta}$$

Besides, it may be clearly seen that the slopes of the shear stress lines are considerably greater than those corresponding to the turbulent normal stresses. This is simple evidence of the fact that the decay of shear stresses in a downstream direction is more intensive than that of normal ones. Now, one may draw the conclusion that the correlation between turbulence velocity components is expected to decrease with the growth of the coordinate \bar{x}_1 . This means that at a sufficiently far distance from the plates the turbulence is supposed to reach the state of isotropy.

One of the particular questions the experiment was to solve was to what extent the development of turbulent stresses could be affected by the value of a longitu-

dinal pressure gradient. The qualitative answer to this may be deduced from the figure already described. However, a clearer interpretation is provided by the data of Fig. 6 where the turbulence stresses — for several fixed control planes $\bar{x}_1 = \text{const}$ — are plotted against the pressure gradient $\partial \bar{p} / \partial \bar{x}_1$.

The empirical results shown here allow one to formulate the following rule: in flows with a negative pressure gradient, that is, in accelerated flows, there is a tendency for the overall turbulence level to decrease; in flows with a positive pressure gradient (retarded flows in space) a tendency is noted towards an increase in turbulence.

This conclusion can also be supported by the turbulence energy equation, which is usually written in the form

$$(3.3) \quad \frac{d}{dt} \left(\frac{\overline{q^2}}{2} \right) = -\overline{u_i u_j} \frac{\partial U_j}{\partial x_i} - \frac{\partial}{\partial x_i} \overline{u_i \left(\frac{p}{\rho} + \frac{q^2}{2} \right)} + \nu \frac{\partial^2}{\partial x_i^2} \overline{q^2} - \nu \overline{\left(\frac{\partial u_j}{\partial x_i} \right)^2}$$

For the two-dimensional shear flow analysed here this relation in the x_1 — direction reads

$$(3.3') \quad \frac{d}{dt} \left(\frac{\overline{q^2}}{2} \right) = -\overline{u_1^2} \frac{\partial U_1}{\partial x_1} - \overline{u_1 u_2} \frac{\partial U_1}{\partial x_2} + \dots$$

Let us consider an accelerated flow ($\partial U_1 / \partial x_1 > 0$); then, the first term in Eq. (3.3') gives a negative contribution to the whole kinetic energy of turbulent motion (in retarded flows the influence of this term is naturally adverse). On the other hand it should be emphasized that the second term of the energy equation — the so-called “production term” responsible for energy transport from the mean to the turbulent motion — always makes a positive contribution to the temporal change in the kinetic energy of turbulence. Its value, however, is supposed to be under the distinct influence of the longitudinal pressure gradient which is experimentally confirmed in Fig. 7 where, for a negative pressure gradient, the energy flux from mean to turbulent motion falls off evidently. And that is undoubtedly the second reason which explains the more intensive decay of turbulence in accelerated flows.

In order to have a more careful look in sight into the changes occurring in the turbulence microstructure under the influence of a longitudinal pressure gradient, let us consider the double correlation coefficient R_{12} between turbulence velocity com-

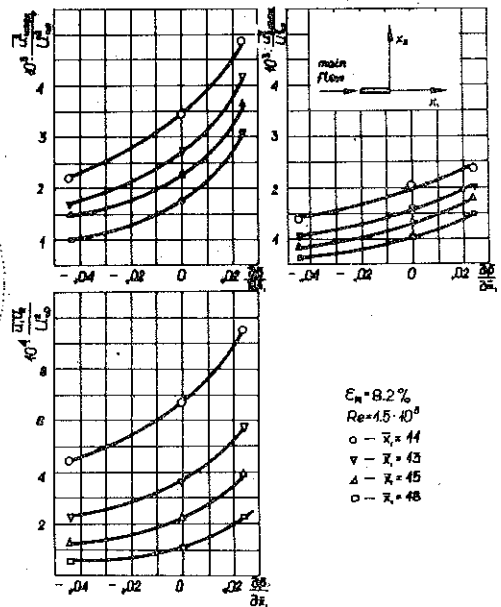


Fig. 6. Turbulence stresses in terms of longitudinal pressure gradient.

ponents. It is worth observing that at a sufficiently far distance from the plates this coefficient — according to Eq. (2.5) — may be expressed as a product of two components

$$R_{1,2} = R_{1,2\max}(\bar{x}_1) F(\eta);$$

the last of them being the universal function of the relative coordinate $\eta = x_2/l(x_1)$. The universal form of this function is shown in Fig. 8 where the coefficient $R_{1,2}$ for several different control planes $\bar{x}_1 = \text{const}$ is plotted in terms of the coordinate η .

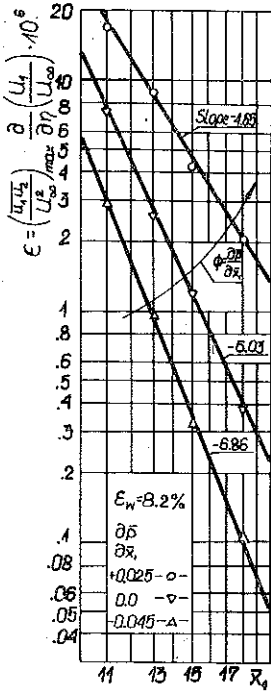


FIG. 7. Energy flux from mean to turbulent motion and its dependence on the quantities \bar{x}_1 and $\partial\bar{p}/\partial\bar{x}_1$.

The evolution of the correlation coefficient in the downstream direction is presented in Fig. 9a. Its decrease according to the growth of the distance \bar{x}_1 reflects the general trend towards the state of isotropy as observed in the majority of turbulent flows.

The influence of pressure gradient on the development of turbulence structure is exhibited in Fig. 9b, where the correlation coefficient is plotted in terms of $\partial\bar{p}/\partial\bar{x}_1$. As it should be remembered from the figures previously shown, all the components of the turbulent stress tensor decrease more rapidly in accelerated flows than in retarded ones. However, the decay of shear stresses is more intensive than the decrease of the normal ones. This indicates that the turbulence structure is closer to isotropy in flows with a negative rather than positive pressure gradient. Moreover, an analysis of the experimental data presented in Figs. 4, 5 and 9a and juxtaposed in Table 1 verifies the thesis previously formulated which claims that the semi-preserving conditions are fulfilled with satisfactory accuracy only for $\partial\bar{p}/\partial\bar{x}_1 = 0$.

A more subtle insight into the problem of turbulence microstructure may be gained through spectral analysis. If we assume the field of turbulence quantities to be quasi-steady, that is, statistically homogeneous with respect to time, we can introduce the concept of energy spectrum tensors E_{ij} or ψ_{ij} which are defined by the relations

$$(3.4) \quad \overline{u_i u_j} = \int_0^\infty E_{ij}(n) dn, \quad \int_0^\infty \frac{E_{ij}(n)}{u_i u_j} dn = \int_0^\infty \psi_{ij}(n) dn$$

and describe the distribution of kinetic energy along all the frequencies existing in turbulent fluctuations.

The exemplary distribution of the relative energy spectrum function ψ_{11} is presented in Fig. 10. The results exposed here concern the given control plane $\bar{x}_1 = 12$ and are related to all the three considered values of the longitudinal pressure gradient.

One can see that the shape of these functions depends strongly on the value of $\partial\bar{p}/\partial\bar{x}_1$ whose growth—that is, the retardation of flow velocity—induces the tendency of energy spectrum to move towards the range of lower wave numbers

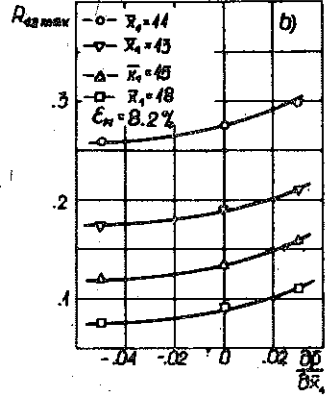
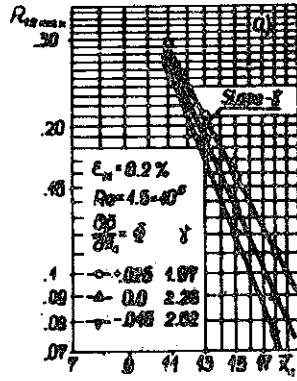
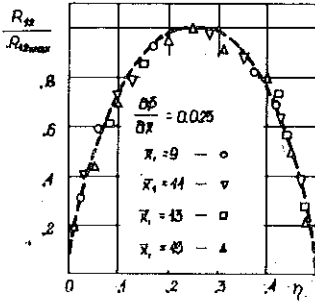


FIG. 8. Universal form of the correlation coefficient.

FIG. 9. The correlation coefficient in terms of the coordinate x_1 (Fig. a) and pressure gradient (Fig. b).

$k=2\pi n/U$ in which the big eddies begin to prevail. The same analysis has been applied to the other components of the energy spectrum tensor. All the results obtained have confirmed the conclusion previously drawn which claims that in retarded flows there is a greater contribution of large eddies responsible for the statistical connection between turbulence velocity components.

Table 1

Experimental data					Semi-preserving conditions	
Relations	$\Delta U_m \sim x^{-2k}$	$U_m^2 \sim x^{-2k}$	$L_m \sim x^{-2\delta}$	$R_{12} \sim x^{-\delta}$	$2\delta - (\beta\ell + 1) = 0$	$2k + \delta - (\beta\ell + 1) = 0$
$\frac{\partial\bar{p}}{\partial\bar{x}_1}$	$\beta\ell$	$2k$	2δ	δ		
+0.025	1.71	0.89	2.78	1.97	0.07	0.15
0.0	2.54	1.32	3.51	2.25	-0.03	0.03
-0.045	2.9	1.6	4.19	2.52	0.29	0.22

The next figure (Fig. 11) demonstrates all the three functions ψ_{ij} determined for a zero pressure gradient $\partial\bar{p}/\partial\bar{x}_1=0$ in the same, fixed point of the velocity field. It is worth noticing that in the range of higher wave numbers the ψ_{12} -function, corresponding to the turbulent shear stresses, decreases more rapidly than the other two ones. To interpret this phenomenon let us introduce now, by analogy to the

overall correlation coefficient R_{12} , the notion of the partial or rather spectral correlation coefficient

$$(3.5) \quad (R_{12})_n = \frac{E_{12}(n)}{[E_{11}(n) E_{22}(n)]^{1/2}}$$

which describes the degree of statistical dependence between longitudinal and lateral fluctuations of the same frequency n . The spectral correlation coefficient determined

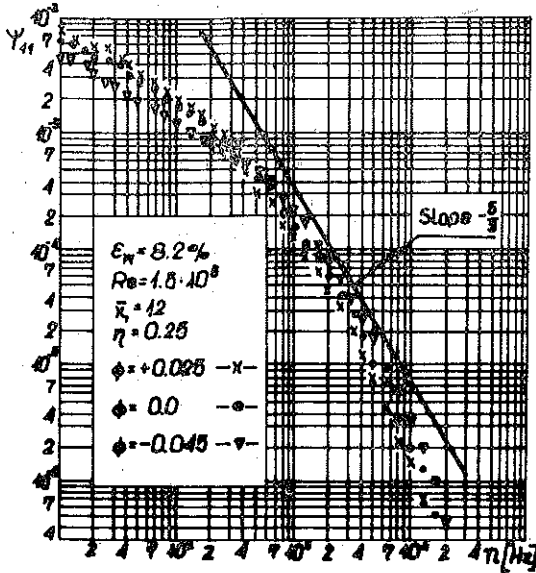


FIG. 10. One-dimensional energy spectrum for different longitudinal pressure gradients.

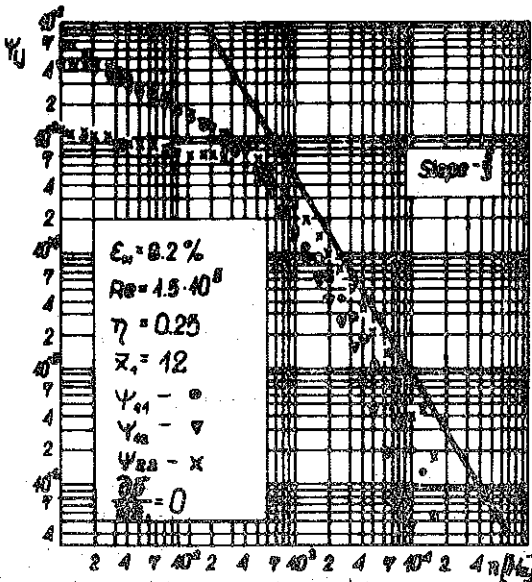


FIG. 11. Energy spectrum functions for a constant value of $\partial \bar{p} / \partial x_1$.

in such a way is plotted in Fig. 12 against frequency n for the three considered values of the pressure gradient. One may observe the distinct influence of $\partial\bar{p}/\partial\bar{x}_1$, the growth of which causes a simultaneous increase of the coefficient $(R_{12})_n$ in the whole tested frequency band. However, this phenomenon becomes quite clear if one only keeps in mind that retarded flows are characterized by a greater contribution of big eddies responsible for the state of anisotropy and that the overall correlation coefficient is a slightly decaying function of the longitudinal pressure gradient.

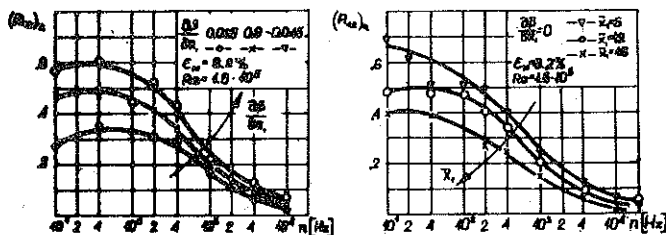


FIG. 12. Spectral correlation coefficient for different values of $\partial\bar{p}/\partial\bar{x}_1$ (Fig. a) and coordinates \bar{x}_1 (Fig. b).

Moreover, it seems to be worth noticing that in the higher frequency range the value of the spectral correlation coefficient decays evidently. It reflects the fact that even in anisotropic turbulent flows the higher wave number range is very close to isotropy; this is in agreement with the hypothesis of local isotropy in the turbulence spectrum as formulated for the first time by Kolmogoroff.

The idea of how the turbulence structure may change with time or with the distance from the plate is given in Fig. 12b where the spectral correlation coefficient has been plotted in terms of the coordinate \bar{x}_1 . According to the statement mentioned above, the correlation between turbulence velocity components decreases in the downstream direction. Its decay is, however, more intensive in the range of higher wave-numbers where the trend to isotropic structure of the smaller eddies is particularly visible.

CONCLUDING REMARKS

The empirical data presented here allow one to formulate the following conclusions:

1. The negative value of the longitudinal pressure gradient accelerates the process of mean velocity field equalization and damps turbulent fluctuations of the flow. Its positive value, characteristic for retarded flows, leads to the growth of the overall turbulence level which results from the decrease of the energy flux ε from mean to turbulent motion.

2. The spectral correlation coefficient $(R_{12})_n$ describing the degree of statistical connection between turbulent fluctuations of a given frequency n is a monotonically

decreasing function of the distance from the cascade plates. Moreover, the coefficient $(R_{12})_n$ decays at a higher rate in accelerated flow than in retarded ones; this means that a negative value of $\partial\bar{p}/\partial\bar{x}_1$ brings the turbulence structure nearer to the state of isotropy.

REFERENCES

1. R. NARASIMHA, A. PRABAU, *Equilibrium and relaxation in turbulent wakes*, I. Fl. Mech., 54 part 1, 1-17, 1972.
2. A. PRABAU, R. NARASIMHA, *Turbulent non equilibrium wakes*, I. Fl. Mech., 54, part 1, 19-38, 1972.
3. P. G. HILL, U. W. SCHAUB, Y. SENOO, *Turbulent wakes in pressure gradient*, Trans. ASME, Ser. E, 4, 1967.
4. R. GRAN OLSSON, *Geschewingekeit und Temperaturverteilung hinter einem Gitter bei turbulenter Stromung*, ZAMM 16, 1936.
5. R. W. STEWART, *An experimental study of homogeneous and isotropic turbulence*, Ph.D. Diss., University of Cambridge, 1951.
6. H. SATO, *On turbulence behind a row of parallel rods*, Proc. 1-st Japan Nat. Congr. Appl. Mech., 1951.
7. H. TAMAKI, K. OSHIMA, *Experimental studies on the wake behind a row of parallel rods*, Proc. 1-st Japan Nat. Congr. Appl. Mech., 1951.
8. J. ELSNER, *Influence of the initial turbulence of flow and the evolution of wakes behind cascade blades*. Arch. Bud. Masz., 15, 3, 1968.
9. J. ELSNER, *A conception of semi-preserving region in cascade flow*, Fluid Dynamics Transaction, 6, part 2.
10. J. ELSNER, *Uogólnione prawo rozwoju pola prędkości w turbulentnym anizotropowym strumieniu palisadowym*, Ciepłn. Masz. Przepł., 71, 1970.
11. A. A. TOWNSEND, *The structure of turbulent shear flow*, Cambridge University Press, 1956.
12. J. WILCZYŃSKI, *Rozwój strugi zapalisadowej z podłużnym gradientem ciśnienia*, D. Diss., Technical University of Częstochowa, 1974.

STRESZCZENIE

EWOLUCJA NAPRĘŻEŃ REYNOLDSA W TURBULENTNYM PRZEPŁYWIE ŚLADOWYM Z PODŁUŻNYM GRADIENTEM CIŚNIENIA

Praca niniejsza dotyczy analizy teoretycznej i doświadczalnej rozkładu naprężeń Reynoldsa w przepływach ze ścinaniem i podłużnym gradientem ciśnienia. Otrzymane wyniki wskazują, że ujemny gradient ciśnienia przyspiesza wyrównywanie średniego pola prędkości i tłumí burzliwe fluktuacje przepływającego ośrodka. Dodatnia wartość wyrażenia $\partial\bar{p}/\partial\bar{x}_1$ wywołuje wzrost całkowitego poziomu turbulencji, który jest wywołany prawdopodobnie wzrostem strumienia energii przenoszonego z ruchu średniego do turbulentnego. Specjalną uwagę poświęcono analizie funkcji spektrum energii i ich zależności od podłużnego gradientu ciśnienia. Wykazano, że spektralny współczynnik podwójnej korelacji pomiędzy składowymi prędkościami turbulentnej jest funkcją rosnącą $\partial\bar{p}/\partial\bar{x}_1$, co należy traktować jako dążność przyspieszanych przepływów do bardziej intensywnej stabilizacji struktury izotropowej.

Резюме

ЭВОЛЮЦИЯ НАПРЯЖЕНИЙ РЕЙНОЛЬДСА В ТУРБУЛЕНТНОМ ТЕЧЕНИИ СО СЛЕДОМ С ПРОДОЛЬНОМ ГРАДИЕНТОМ ДАВЛЕНИЯ

Настоящая работа касается теоретического и экспериментального анализа распределения напряжений Рейнольдса в течениях со сдвигом и продольным градиентом давления. Полученные результаты показывают, что отрицательный градиент давления ускоряет выравнивание среднего поля скорости и тушит турбулентные флуктуации протекающей среды. Положительное значение выражения $\partial \bar{p} / \partial \bar{x}_1$ вызывает рост полного уровня турбулентности, который вызывается вероятно ростом потока энергии переносимого из среднего в турбулентное движение. Специальное внимание посвящено анализу функции спектра энергии и его зависимости от продольного градиента давления. Показано, что спектральный коэффициент двойной корреляции между составляющими турбулентной скорости является функцией $\partial \bar{p} / \partial \bar{x}_1$ что следует трактовать как стремление ускоряемых течений к более интенсивной стабилизации изотропной структуры.

Received October 30, 1975.
